Available online at www.sciencedirect.com

SciVerse ScienceDirect

Procedia CIRP 8 (2013) 444 – 449

www.elsevier.com/locate/procedia

14th CIRP Conference on Modeling of Machining Operations (CIRP CMMO)

Modeling of delamination during milling of unidirectional CFRP

Wolfgang Hintze*, Dirk Hartmann

Hamburg University of Technology, Institute of Production Management and Technology, Denickestraße 17, 21071 Hamburg, Germany

* Corresponding author. Tel.: +49-40-42878-3051; fax: +49-40-42878-2295. w.hintze@tu-harburg.de.

Abstract

The production of CFRP needs edge trimming in order to remove burrs as well as undefined orientated fibres and to shape the final part contour. Edge trimming is usually done by contour milling. The quality of machined edges may be affected by fibre protrusions and delaminated fibres which cause manual repair or may even lead to scrap.

Delamination of fibres is often initiated by stresses applied during engagement of the cutting edge. Based on measured cutting forces, the stress distribution and the inter fibre fracture modes in the boundary zone of the machined surface are calculated using Lekhnitskii's theory of elasticity for anisotropic elastic bodies and the fracture criteria of Puck.

In course of the continuing edge trimming process, fibre ends in the damaged boundary zone might not be cut off but deflected by subsequent tool engagements, as can be observed in high speed videos. In the case of existing fibre protrusions, a relation between the minimum depth of the damaged zone, the fibre orientation at the machined edge and the fibre properties was derived using elementary bending models. The analysis underlines the existence of only one type of surface ply delamination i.e. fibre protrusions and fibre delamination always occur together.

Selection and peer-review under responsibility of The International Scientific Committee of the "14th CIRP Conference on Modeling of Machining Operations" in the person of the Conference Chair Prof. Luca Settineri

Keywords: CFRP; milling; delamination; theory of elasticity

1. Introduction

Delamination is a major production error when machining fibre-reinforced plastics. In connection with the milling of CFRPs, delamination is generally recognised as the damaging of laminate top layers. Chipping and protruding fibres are signs of this type of delamination. Delaminated components make the assembly process more difficult and their mechanical properties are impaired [1, 2]. Delamination causes reworking, which costs both time and money or even leads to scrap. An overall understanding of the delamination process helps to specifically avoid delamination.

While delamination during drilling is the subject of numerous scientific studies and diverse model approaches have been developed to describe it [2, 3, 4], the subject of contour milling has to date received less literary interest [5, 6, 7, 8, 9]. However we do know that delamination depends decisively on the tool wear and the alignment of the fibre to the cutting direction of the tool – hereinafter referred to as the fibre cutting angle θ - and that under standard conditions, even in the case of polycrystalline diamond tools, the cutting edge radius r_β increases very rapidly due to wear [5, 6, 8, 10]. The mechanisms for the development and propagation of delamination have been described by the authors in [9, 11].

The cause of the development of delamination is the stress in the cutting area due to the cutting force induced by the acting tool. The stress load can be calculated using Lekhnitskii's theory of elasticity for anisotropic elastic bodies [8, 12, 13, 14]. Puck formulated inter fibre fracture criteria for the breakdown of fibre composites depending on stress conditions [15].

The aim of the study is to schematically describe the development and propagation of delamination during contour milling under practical conditions. Delamination is especially pronounced in CFRP laminates with unidirectional top layers. Therefore milling using unidirectional CFRP sheets with different fibre alignments and under practical tool wear, i.e. a cutting edge radius of r_β = 90μm is looked at. In compliance

Selection and peer-review under responsibility of The International Scientific Committee of the "14th CIRP Conference on Modeling of Machining Operations" in the person of the Conference Chair Prof. Luca Settineri
doi:10.1016/j.procir.2013.06.131

with conventional tool geometry it is assumed that the back rake or cutting inclination angle is $\gamma_p = \lambda_s = 0°$.

The relevant cutting force F is the result of a removal mechanism that includes separation of fibre bundles, shattering of fibres at the cutting surface and friction effects. It has as such not yet been subject to satisfactory modeling [16, 17]. The modeling of the delamination process during contour milling therefore emanates from measured cutting forces [7]. Due to $\lambda_s = 0°$ there is no passive force and the cutting force corresponds to the active force: $F = F_a$.

2. Modeling of the initial boundary zone damage as a result of the cutting action

To model the initial damage on the cutting surface of unidirectional (orthotropic) CFRP material using the cutting force, it is assumed that the active force measured acts as a constant line force on a surface, resulting from the cutting edge radius r_β and the depth of cut or laminate thickness $a_p = b$, Fig. 1. Variation calculus has shown that the calculated stress distribution is only slightly influenced [8] by the assumed (rectangular or triangular) load distribution.

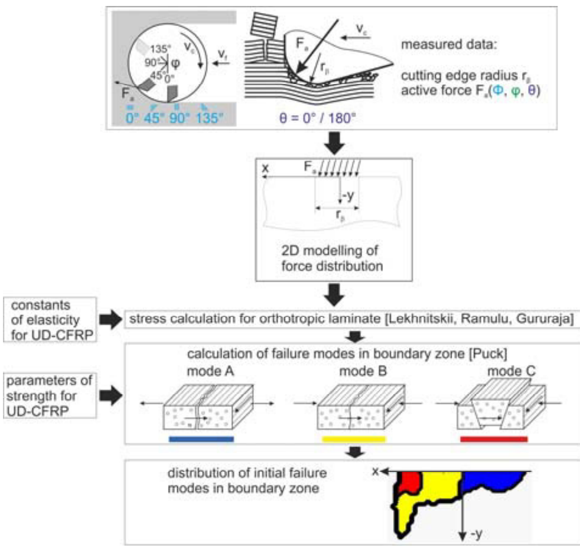

Fig. 1: Modeling and calculation of initial failure of the boundary zone.

The stress distribution in the boundary zone under the cutting surface is determined from the line load according to the known approach for orthotropic materials [12]. Thereby, the elastic material constants of the UD-CFRP (Youngs moduli $E_\perp$, E_{II}, shear moduli $G_{\perp II}$, $G_{\perp\perp}$, Poisson ratios $\nu_{\perp II}$, $\nu_{\perp\perp}$) are taken into account.

Based on the stress distribution, the inter fibre fracture criteria of Puck [15] decisive for the damage modes A to C are subsequently calculated. The strength parameters for UD-CFRP ($R_{\perp\parallel}$, $R_\perp^+$, $R_\perp^-$, $R_{\perp\perp}^A$, τ_{21c}, $p_{\perp\parallel}^+$, $p_{\perp\parallel}^-$) are considered here. The result is the local distribution of the damage modes in the boundary zone.

During milling of UD-CFRP the active force F_a changes by means of the engagement angle φ of the cutting edge and depending on the fibre orientation angle ϕ with respect to the feed direction (v_f). From φ and ϕ the fibre cutting angle θ can be clearly determined, this in turn defines the angle between the fibres and the cutting direction (v_c) [18] and is crucially important for the delamination process [9]:

$$\theta = \varphi + \phi; \qquad 0° \leq (\varphi + \phi) \leq 180° \tag{1}$$

$$\theta = \varphi + \phi - 180°; \qquad 180° < (\varphi + \phi) < 360° \tag{2}$$

As an example, the local distribution of the initial damage was calculated during contour milling for a unidirectional CFRP laminate for $\phi = 135°$ and for $\varphi = 45°$, 90°, 135° corresponding to $\theta = 0°$, 45°, 90°, Fig. 2.

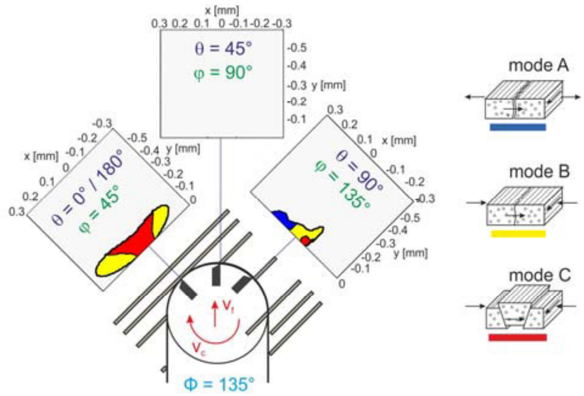

Fig. 2: Distribution of initial failure modes.

The elastic constants and strength parameters for the CFRP material are listed in table 1. The tool parameters and cutting conditions are listed in table 2 together with the cutting and cutting normal forces F_c (ϕ =135°, φ or θ) and F_{cn} (ϕ =135°, φ or θ) measured at three engagement and fibre cutting angles respectively. Literature on the HT-fibres and the epoxy resin were used as references for the material properties [1, 15, 19]. Due to the required time resolution for a dynamic measurement of the cutting force the tests were carried out at a low cutting speed v_c.

In the case of the fibre cutting angles $\theta = 0°$ and 90°, the calculated initial damage of the boundary zone stretches to a depth of $\Delta_i = 0.1$ to 0.2mm, while at $\theta = 45°$ despite a high level of tool wear no initial damage was determined. This result is in line with experimental findings [9]. The damage modes A and C are particularly critical as they cause single fibres to peel away or laminate layers to separate.

Table 1: Material data 1) of unidirectional Cytec HTS 977-2 and 2) from [15]

Youngs modulus E_{II} [N/mm^2] 1)	139360
Youngs modulus $E_{\perp}$ [N/mm^2] 1)	8800
shear modulus $G_{\perp\perp}$ [N/mm^2] 1)	3200
shear modulus $G_{\perp II}$ [N/mm^2] 1)	4600
Poisson ratio $\nu_{\perp II}$ [-] 1)	0.29
Poisson ratio $\nu_{\perp\perp}$ [-] 1)	0.37
shear strength $R_{\perp\parallel}$ [N/mm^2] 2)	80
tensile strength $R_{\perp}^{+}$ [N/mm^2] 2)	60
compressive strength $R_{\perp}^{-}$ [N/mm^2] 2)	180
fracture strength of the action plane $R_{\perp\perp}^{A}$ [N/mm^2] 2)	75
fracture strength parameter τ_{21c} [N/mm^2] 2)	90
inclination parameter $p_{\perp\parallel}^{+}$ 2)	0,3
inclination parameter $p_{\perp\parallel}^{-}$ 2)	0,2

The initial damage zones were determined in the same way for the fibre orientation angles ϕ = 0°, 45° and 90°. The determined damage depths are shown according to mode C in Fig. 3. The measured force components, on which the calculations are based, are also listed in table 2 [8].

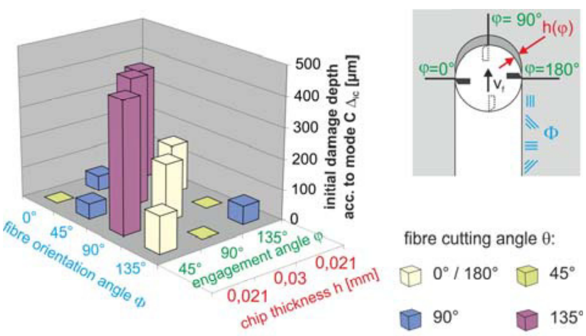

Fig. 3: Depth of the initial damage zone Δ_{iC} caused by inclined inter fibre fracture (mode C).

It can be observed that the fibre cutting angle θ compared with the fibre orientation angle ϕ and the engagement angle φ or the cutting thickness h has a dominant influence on the initial damage depth according to mode C, denoted by Δ_{iC}. Regardless of ϕ, φ or h the calculations at θ = 45° display no damage, while at θ = 135° Δ_{iC} range up to 0.45 mm.

Table 2: Measured cutting and cutting normal forces depending on ϕ and φ or θ.

ϕ [°]	φ [°]	h [mm]	θ [°]	F_c [N]	F_{cn} [N]
0	45	0.02	45	-4.4	69.9
	90	0.03	90	105.5	264.1
	135	0.02	135	156	489.3
45	45	0.02	90	99,3	260.4
	90	0.03	135	168.7	559.6
	135	0.02	180/0	81.8	318.9
90	45	0.02	135	148.3	569.2
	90	0.03	180/0	76.5	375.7
	135	0,02	45	8,9	15.8
135	45	0,02	180/0	61.5	263.3
	90	0,03	45	0	60.9
	135	0,02	90	108.6	259.2
tool geometry $\gamma_f = 0°$, $\alpha_f = 12°$, $\gamma_p = 0°$, z = 2, r_β = 90 µm					
parameters n = 100 min^{-1}, v_f = 6 mm/min (f_z = 0.03 mm) $a_e = d_{tool}$ = 12,7 mm, a_p = 4 mm					
material Cytec HTS 977-2, unidirectional					

3. Modeling of the boundary zone damage in the case of fibre protrusions

Numerous experimental studies have shown that contour milling with blunt tools leads to damage of the top layers due to delamination and to fibres protruding over the edge of the manufactured component [5, 6, 8, 20, 4]. High-speed videos show that fibres or fibre bundles can repeatedly avoid the tool during its feed motion, Fig. 4. Simplifying this process to the extreme cases, the fibres or bundles are bent either in the laminate plane or perpendicular to it.

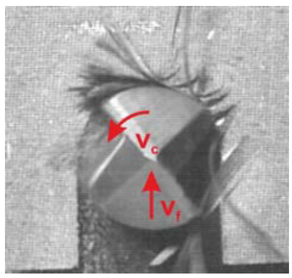

Fig. 4: High-speed video of contour milling showing deflected fibre bundles.

The reason why the fibres deflect without being broken is that their transverse rupture strain is not attained. A minimal fibre curvature radius $r_{min\ f}$ is decisive to attain the transverse rupture strain. Applying an equation on the ultimate tensile strain ε_B, known from sheet metal forming [21], $r_{min\ f}$ depends on ε_B and on the fibre diameter d_{fibre}:

$$r_{\min\_f} = \frac{1}{2} \cdot \left(\frac{1}{\varepsilon_B} - 1 \right) \cdot d_{fibre} \quad (3)$$

In the case of HTS or IMS fibres the values ε_B, d_{fibre} and r_{min_f} are listed in table 3.

Table 3: Minimal fibre curvature radius of HTS and IMS fibres

	ε_B [%]	d_{fibre} [µm]	r_{min_f} [µm]
HTS	1,8	7	191
IMS	1,9	5	129

This approach applies as far as the fibres are totally separated from each other. In fact, they are often separated in bundles of the top laminate layer. The bundle widths vary in a wide range depending on the cutting conditions [9]. However, the bundle thickness is given by the laminate thickness t_{lam}. As a first approximation t_{lam} is taken as the relevant dimension for bending of fibre bundles. Assuming the fibre bundles as ideal elastic and substituting d_{fibre} by the laminate thickness t_{lam}, the minimal curvature radius of fibres bundles r_{min_b} is obtained accordingly, see table 4.

Table 4: Minimal curvature radius of HTS and IMS fibre bundles.

	ε_B [%]	t_{lam} [µm]	r_{min_b} [µm]
HTS	1,8	250	6822
IMS	1,9	250	6450

Using the minimal curvature radii both swerve mechanisms can be modeled. Fig. 5 shows schematically how the fibres avoid the tool in the laminate plane for the selected fibre cutting angle θ.

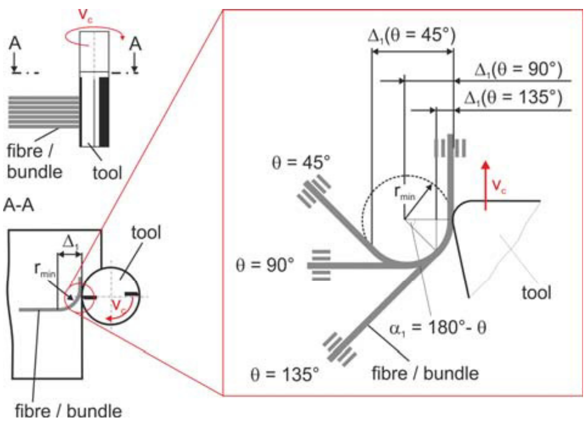

Fig. 5: Bending of fibres or bundles in the laminate plane.

To ensure that the fibres bend around the radius r_{min_f} they must move freely at a depth Δ_{1_f}, i.e. they must be delaminated. Δ_{1_f} is calculated according to figure 5:

$$\Delta_{1\_f} = r_{\min\_f} \cdot (1 + \cos\theta) + d_{fibre} \quad (4)$$

The minimum required damage depth Δ_{1_f} for the fibres to deviate in the laminate plane depends therefore on the minimum curvature radius of the fibres r_{min_f}, on the fibre cutting angle θ and on the fibre diameter d_{fibre}. The according relationship for the required damage depth Δ_{1_b} for bundles is approximately calculated by

$$\Delta_{1\_b} = r_{\min\_b} \cdot (1 + \cos\theta) + t_{lam} \quad (5)$$

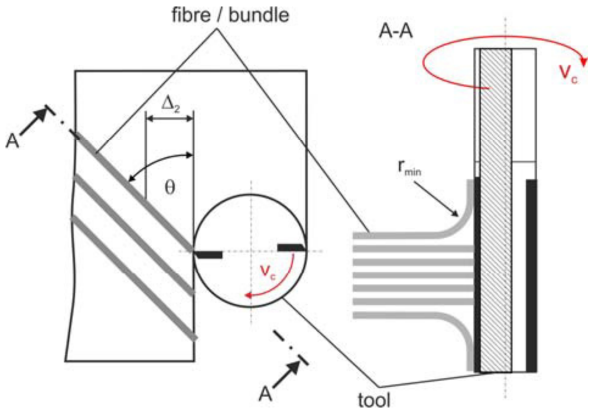

Fig. 6: Bending of fibres or bundles perpendicular to the laminate plane.

Fig. 6 shows schematically how the fibres or bundles avoid the tool perpendicular to the laminate plane. It is assumed that the tool moving along the feed path represents a level obstacle for protruding fibres or bundles. They contact it at the fibre cutting angle θ. To ensure that the fibres or bundles bend at this angle around the respective radius r_{min}, they must move freely at a depth Δ_2, i.e. be delaminated at a depth Δ_2 from the component edge. According to figure 6, Δ_{2_f} can be calculated from θ, r_{min_f}, d_{fibre} and Δ_{2_b} calculated from θ, r_{min_b}, t_{lam} respectively:

$$\Delta_{2\_f} = r_{\min\_f} \cdot \sin\theta + d_{fibre} \quad (6)$$

$$\Delta_{2\_b} = r_{\min\_b} \cdot \sin\theta + t_{lam} \quad (7)$$

In Fig. 7 minimal damage depths Δ_1 und Δ_2 connected to both deviation mechanisms and depending on the fibre cutting angle θ for HTS fibres and bundles are presented. In accordance with experimental observations the depths Δ_{1_b} und Δ_{2_b} obtained for deflected bundles are much higher than those for fibres. At fibre cutting angles 0° < θ < 90° the deflection of fibres or bundles occurs preferably perpendicular to the laminate plane, because this mechanism requires the smaller depth $\Delta_2 < \Delta_1$ at given r_{min}. For 90° < θ < 180° bending in the laminate plane is relevant because of $\Delta_1 < \Delta_2$. Due to smaller r_{min} values IMS fibres can avoid the tool at smaller depths Δ_1 and Δ_2 than HTS fibres.

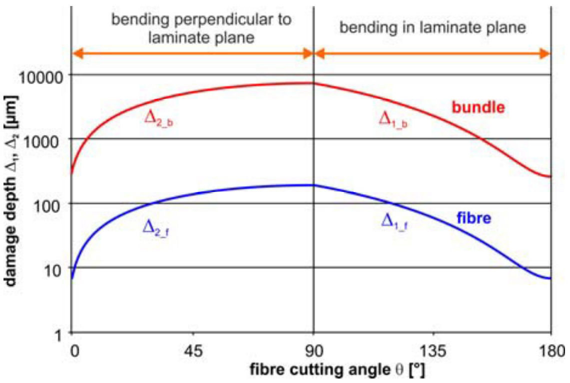

Fig. 7: Minimal damage depths due to fibre and bundle deflection and relevant bending mechanisms for HTS.

It should also be considered that the frictional force applied through the rotating tool on the protruding fibres or bundles promotes their deviation in the laminate plane. On the other hand the deviation of the fibres or bundles perpendicular to the laminate plane is favoured in tools with positive back rake or inclination angle $\gamma_p = \lambda_s > 0°$. A negative angle $\gamma_p = \lambda_s < 0°$ effectively hinders or suppresses the deviation mechanism perpendicular to the laminate plane in a range 0° < θ < 90°, where $\Delta_2 < \Delta_1$. The deviation of the fibres can therefore not be exclusively assigned in practice to one mechanism.

4. Influence of initial boundary zone damage on fibre protrusions and top layer delamination

The comparison of the initial damage depths Δ_{iC} with the minimum damage depths due to fibre or bundle deflections Δ_1 and Δ_2 (comp. figures 3, 7 and tables 1, 2) indicates how fibre and bundle protrusions and top layer delamination occur and propagate. The depth values depending on the fibre cutting θ are summarized in Fig. 8.

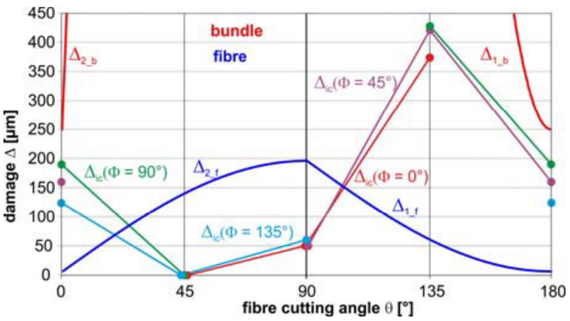

Fig. 8: Initial damage depths Δ_{iC} and minimum damage depths Δ_1, Δ_2.

Provided that the initial damage depth Δ_{iC} is less than the required minimum damage depth for fibre deflection $(\Delta_{1\_f},\Delta_{2\_f})_{min}$, the fibres will be cut off through the subsequent tool engagement. This is true for initial damage depths Δ_{iC} measured at θ = 45°or 90°. In the opposite case fibre protrusions occur or increase at θ = 135° or 0°/180°. Because Δ_{iC} is less than the required minimum damage depth for fibre bundle deflection $(\Delta_{1\_b},\Delta_{2\_b})_{min}$ at any θ values, bundles will not be generated by the initial tool engagement.

Once delamination of fibres is initiated at a certain θ it may propagate during repeated tool contacts and extend to fibre bundles encompassing even fibre cutting angles θ that are initially damage free. The underlying mechanisms were presented in [8, 9].

In order to avoid delamination development during edge trimming the initial damage depths Δ_{iC} caused by the cutting forces should be restricted such that for all fibre cutting angles θ during tool engagement Δ_{iC} is kept below the minimum damage depths for fibre deflection $\Delta_{iC} < (\Delta_{1\_f},\Delta_{2\_f})_{min}$. This request determines suitable cutting parameters as well as the admissible tool wear.

5. Summary and outlook

Top layer delamination is a crucial quality issue in CFRP machining.

An analytical model for the development of fibre protrusions and top layer delamination in contour milling of unidirectional CFRP has been derived: Geometric and mechanical properties of orthotropic CFRP laminates are considered as well as the effective tool geometry and its varying orientation with respect to the fibres, defined by the fibre cutting angle θ. Cutting conditions and tool wear are taken into account by measured active forces.

The following findings have been obtained:

- The active force leads to initial damage of the laminate which can cause fibres to deflect instead of being cut off
- Two deflection mechanisms of fibre protrusions can be distinguished.
- Any fibre protrusion at machined edges is associated with delamination
- Protruding fibre bundles lead to much deeper top layer delamination than protrusions of separate fibres.

The model is applicable for any CFRP laminate with unidirectional top layers. It can be used in the future to deduce the limits for permissible cutting force or tool wear.

References

[1] Gordon, S.; Hillery, M.T, 2003, A review of the cutting of composite materials, Proc. Instn. Mech. Engrs Vol. 217 Part L: J. Materials: Design and Applications, 217/L:35-45.

[2] Sheik-Ahmad, J. Y., 2009, Machining of Polymer Composites, Springer-Verlag.

[3] Tsao, C.C.; Hocheng, H., 2007, Effect of tool wear on delamination in drilling composite materials, International Journal of Mechanical Sciences 49:983-988

[4] Paulo Davim, J., 2010, Machining Composite Materials, John Wiley & Sons

[5] Colligan, K.; Ramulu, M., 1991, Delamination in surface plies of Graphite/Epoxy caused by the Edge Trimming Process, Processing and Manufacturing of Composite Materials 27.

[6] Colligan, K.; Ramulu, M., 1992, The Effect of Edge Trimming on Composite Surface Plies. Manufacturing Review, 5/4:274–283.

[7] Hintze, W.; Hartmann, D.; Goßmann, U., 2012, Kantenqualität beim Umrissfräsen von CFK verbessern, VDI-Z 1/2:24-27.

[8] Hartmann, D., 2012, Delamination an Bauteilkanten beim Umrissfräsen kohlenstofffaserverstärkter Kunststoffe, Dissertation, Hamburg, TUHH.

[9] Hintze, W.; Hartmann, D.; Schütte, C., 2011, Occurrence and propagation of delamination during the machining of carbon fibre reinforced plastics (CFRPs) – An experimental study, Composite Science and Technology, 71/15:1719–1726.

[10] Kindler, J., Werkstückqualität und Standzeitoptimierung von Zerspanwerkzeugen bei der Umrissbearbeitung von kohlenstofffaserverstärkten Kunststoffen, 2010, Dissertation, Hamburg, TUHH.

[11] Hintze, W.; Hartmann, D.; Schütte, C., 2011, Verfahren zum Fräsen von langfaserverstärkter Verbundkunststoffen, PCT-Anmeldung WO 2011/085949 A1.

[12] Lekhnitskii, S.G., 1963, Theory of elasticity of an anisotropic elastic body, Holden Day.

[13] Gururaja, S.; Ramulu, M., 2007, Stress distribution due to inclined line loads in fiberous polymer composites, ICCES, 4/2:73-80.

[14] Gururaja, S.; Ramulu, M., 2009, Failure Analysis of fibrous composite half-space subjected to uniform surface line load, Journal of engineering materials and technology, 131:1-8.

[15] Puck, A., 1996, Festigkeitsanalyse von Faser-Matrix-Laminaten - Modelle für die Praxis, Carl Hanser Verlag.

[16] Hintze, W.; Clausen, R; Hartmann, D.; Kindler, J.; Santos, S.; Schwerdt, M.; Stöver, E., 2007, Precision of machined CFRP - The challenge of dimensional accuracy, Proceedings of the 1st International Workshop on Aircraft System Technologies (AST 2007), Shaker Verlag Aachen, 361-374.

[17] Rentsch, R.; Pecat, O.; Brinksmeier, E., 2011, Macro and micro process modeling of the cutting of carbon fiber reinforced plastics using FEM, Procedia Engineering, 10:1823-1828.

[18] Hohensee, V., 1992, Umrissbearbeitung faserverstärkter Kunststoffe durch Fräsen und Laserschneiden, Dissertation, Aachen, RWTH.

[19] Schürmann, H., 2007, Konstruieren mit Faser-Kunststoff-Verbunden, Springer-Verlag.

[20] Teti, R., 2002, Machining of Composite Materials, Annals of the CIRP, 51/2:611-634

[21] Lange, K., 1990, Umformtechnik, Band 3: Blechbearbeitung, Springer-Verlag.